AGU PUBLICATIONS

Geophysical Research Letters

RESEARCH LETTER
10.1002/2015GL065177

Key Points:
- First observation of charged nanograins from a comet
- Nanograins are reflected by solar radiation pressure and accelerated by solar wind electric fields
- Nanograins return to the vicinity of the comet after significant energization

Correspondence to:
J. L. Burch,
jburch@swri.edu

Citation:
Burch, J. L., T. I. Gombosi, G. Clark, P. Mokashi, and R. Goldstein (2015), Observation of charged nanograins at comet 67P/Churyumov-Gerasimenko, *Geophys. Res. Lett.*, *42*, 6575–6581, doi:10.1002/2015GL065177.

Received 30 JUN 2015
Accepted 5 AUG 2015
Accepted article online 21 AUG 2015
Published online 31 AUG 2015

Observation of charged nanograins at comet 67P/Churyumov-Gerasimenko

J. L. Burch[1], T. I. Gombosi[2], G. Clark[3], P. Mokashi[1], and R. Goldstein[1]

[1]Southwest Research Institute, San Antonio, Texas, USA, [2]AOSS Department, University of Michigan, Ann Arbor, Michigan, USA, [3]The Johns Hopkins University Applied Physics Laboratory, Laurel, Maryland, USA

Abstract Soon after the Rosetta Orbiter rendezvoused with comet 67P/Churyumov-Gerasimenko at a solar distance of ~3.5 AU and began to fly in triangular-shaped trajectories around it, the Ion and Electron Sensor detected negative particles at energies from about 100 eV/q to over 18 keV/q. The lower energy particles came from roughly the direction of the comet; the higher-energy particles came from approximately the solar direction. These particles are interpreted as clusters of molecules, most likely water, which we refer to as nanograins because their inferred diameters are less than 100 nm. Acceleration of the grains away from the comet is through gas drag by the expanding cometary atmosphere, while acceleration back to the vicinity of the comet is caused partly by solar radiation pressure but mainly by the solar wind electric field. These observations represent the first measurements of energetic charged submicron-sized dust or ice grains (nanograins) in a cometary environment.

1. Introduction

As a comet approaches the Sun, solar insolation produces an expanding atmosphere through heating and sublimation of water vapor and other volatile elements and compounds that were previously adsorbed on the surface of its nucleus or perhaps more likely that originate below the surface. In the process, some of the smaller dust and icy conglomerates on the surface are dragged away by the expanding atmosphere. Photoionization by the Sun, particle impact by the solar wind, and collection of cometary electrons produce a partially ionized gas with embedded dust and ice grains, i. e., an expanding dusty plasma. Our interest here is in the smaller-sized dust or ice grains, which we refer to as nanograins (diameters of up to hundreds of nanometers). The charge on the grains is determined by photoemission, electron collection, and secondary emission currents [cf. *Horányi and Mendis*, 1985]. At the large distance from the Sun of comet 67P/Churyumov-Gerasimenko (67P) during these observations (~3.5 AU) it might be expected that electron collection dominates because of the ~R^{-2} dependence of solar UV irradiance and solar wind flux [*Köhnlein*, 1996] combined with the generally $>100\,\mathrm{cm}^{-3}$ electron densities observed close to the comet (~10 km), which decrease only linearly with distance [*Edberg et al*., 2015]. The grains should therefore be mostly negatively charged, and this conclusion is possibly borne out by the fact that the spacecraft potential during this phase of the mission was also generally negative [*Edberg et al*., 2015; *Burch et al*., 2015].

As the nanograins are carried outward by the drag forces of the expanding atmosphere, they eventually reach a terminal velocity of a few hundred m/s at some tens of kilometers above the comet [cf. *Gombosi et al*., 1986, 2015]. From this point on, the nanograin trajectories are influenced mainly by solar radiation pressure and the solar wind electric field (gravitational effects are negligible by comparison). Analysis of such trajectories by *Horányi and Mendis* [1985] showed that solar radiation pressure produces parabolic ballistic trajectories. These trajectories are modified by the solar wind electric field, which becomes more important for smaller particles and less important for the larger ones. Since radiation pressure forces on the particles are conservative, they produce simple reflection so that near the nucleus the returning particles have the same velocities (the terminal velocities) they had when they left the comet. However, changes of the charge state of the nanograins (e.g., by photoionization or electron collection) or of their masses (e.g., by breakup) as suggested by *Gombosi et al*. [2015] could change the energy/charge at which they are detected by an electrostatic analyzer.

In August 2014, *Rosetta* rendezvoused with comet 67P and commenced a series of maneuvers that took it on two successive triangular paths (averaging 100 and 50 km from the nucleus, respectively) whose segments

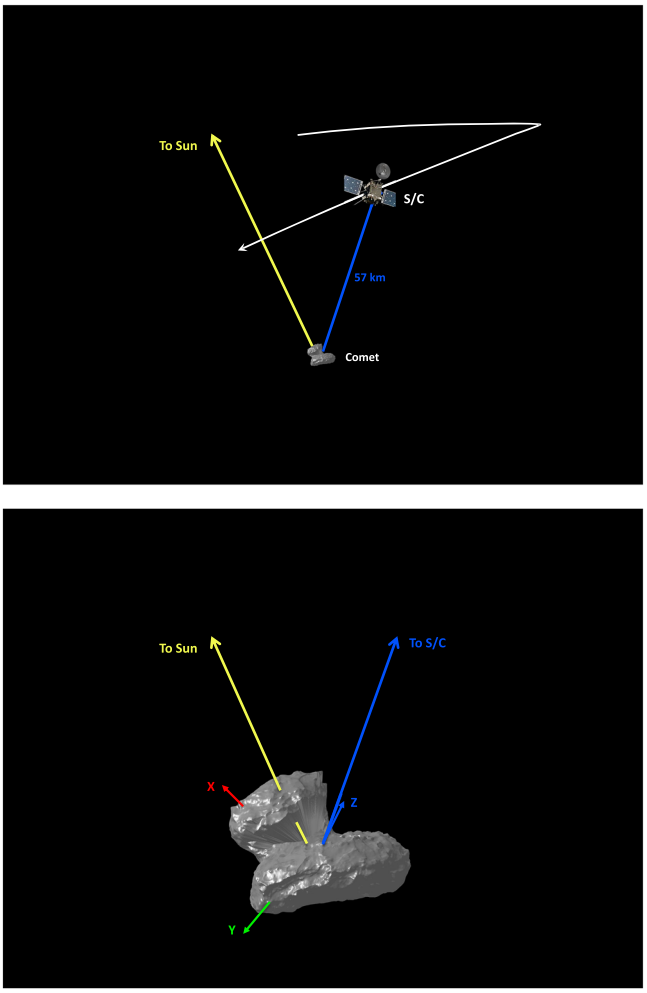

Figure 1. Position of Rosetta on 30 August 2014 at 0613 UT. (a) Triangular path of Rosetta (white), line to the Sun (yellow), and line to the spacecraft (blue). (b) Close-up view of the nucleus shape model showing lines to the Sun and the spacecraft along with cartesian vectors *x* (red), *y* (green), and *z* (blue) in the J2000 system (heliocentric inertial frame at epoch 1 January 2000). For scale, the comet-spacecraft distance is ~57 km and the long axis of the comet is ~5 km. Diagrams are provided by the "3d Tool" developed by the European Space Agency's Rosetta Project.

are hyperbolic escape trajectories alternating with thruster burns. The observations of charged nanograins reported in this paper were made at cometocentric distances between 50 and 65 km on the dayside of 67P between 23 August and 1 September 2014. Figure 1 shows the trajectory, the spacecraft position, and the directions to the Sun and comet on 30 August 2014 at 0613 UT, which is typical for all four events studied.

2. Instrumentation and Data

The Ion and Electron Sensor (IES) on the Rosetta Orbiter measures ions and electrons with energy/charge from 4 eV to 18 keV with 8% energy resolution and 5°×22.5° angular resolution for electrons and 5°×45° for ions, with the ion sector normally containing the solar wind segmented into nine 5°×5° channels [*Burch et al.*, 2007]. Because of the low data rates available (~265 bits/s in burst mode), averaging over adjacent energy and/or angular channels is typically necessary. Since Rosetta is a three-axis stabilized spacecraft with no scan platform, IES performs electrostatic scanning of its intrinsic 5°×360° azimuthal field of view (FOV) over ±45° yielding sixteen 5° elevation angle channels and a total FOV of 2.8π sr. This geometry leads to a fan-shaped field of view for zero elevation angle but to one that lies along the surface of a cone for positive or negative elevation angles. IES is mounted on a corner of the spacecraft with the symmetry axis of the toroidal top hat analyzers centered on a 45° angle from the local spacecraft zenith in order to maximize viewing of both the solar wind and the comet for most anticipated spacecraft orientations. While this objective is generally achieved, there are unavoidable obstructions for some azimuths at certain elevation angles that graze the spacecraft. These obstructions are kept in mind and avoided during data analysis.

3. Observations

Figure 1a shows the triangular-shaped trajectory of the Rosetta Orbiter (white trace) along with lines from the comet to the Sun (yellow) and to the spacecraft (blue). Figure 1b shows a close-up view of a nucleus shape model with the same lines toward the Sun and the spacecraft along with *x* (red), *y* (green), and *z* (blue) vectors in the J2000 coordinate system [*Tapley et al.*, 2004]. Figure 1 is typical for the four events studied since for the entire period from 23 August to 1 September the spacecraft was moving slowly (a few m/s relative to the comet) along the same triangular path while staying on the dayside at comet distances between 50 and 60 km. In each case the line from the comet to the spacecraft originates in

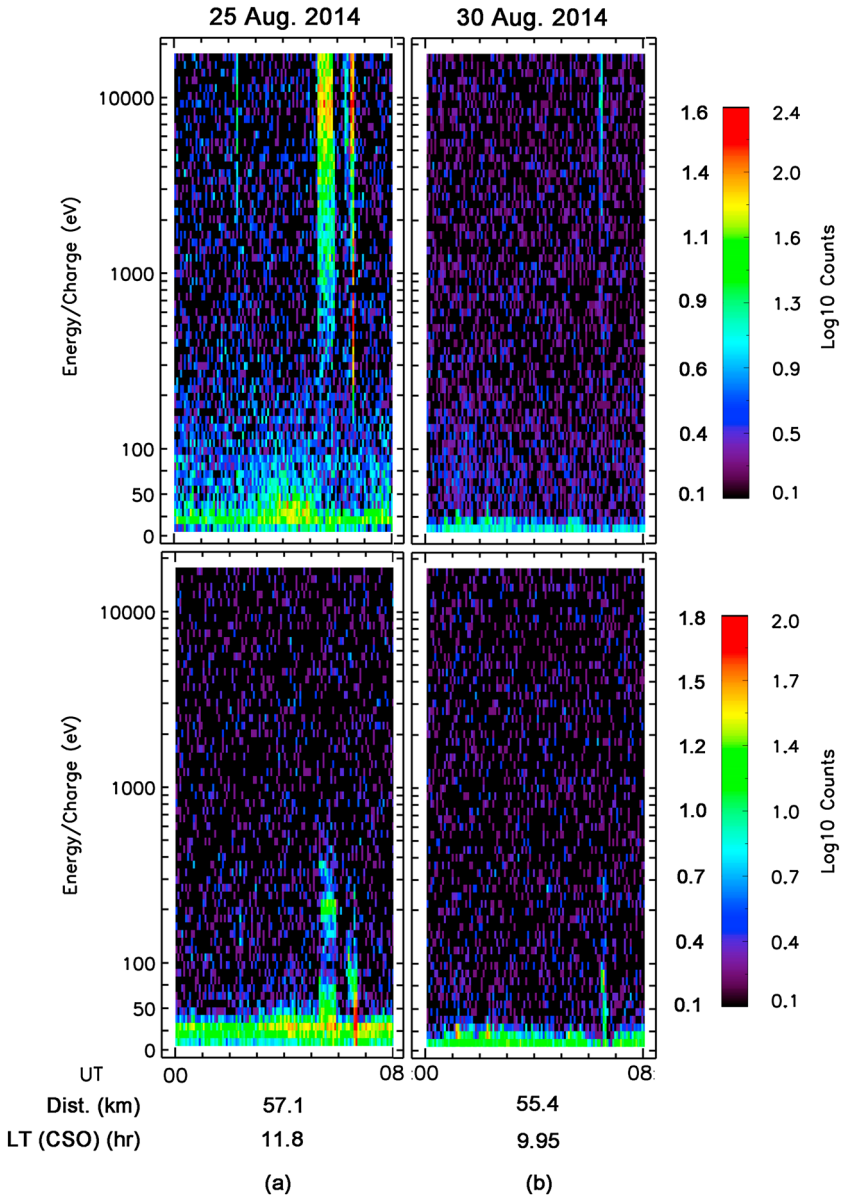

Figure 2. Energy-time spectrograms for negative particles on (a) 25 August and (b) 30 August 2014. Data are from elevation angles 0 and 1 and for anodes 8 and 9 (top plots) and anodes 0 and 1 (bottom plots). Count rates noted on the left- and right-hand sides of the color bars are for 25 and 30 August, respectively.

the neck region of the comet from which plumes of gas and dust have often been observed by the Rosetta navigation camera (e.g., http://blogs.esa.int/rosetta/2014/10/02/cometwatch-26-km-on-26-september/).

Figure 2 shows energy-time spectrograms from the IES electron analyzer for (a) 25 August and (b) 30 August 2014. On these days two adjacent energy channels, two adjacent 5° elevation angle channels, and two adjacent 22.5° polar angle (or azimuth) channels were averaged in order to fit the available telemetry rate. The spectrograms plot $\log_{10}$(counts/0.38 s) at 62 energy steps. For an electrostatic analyzer like IES count rate is proportional to energy flux. These two events are typical of the four events analyzed in this study.

The events of interest occur between 05 and 06 UT in Figure 2a and between 06 and 07 UT in Figure 2b. In each case the upper spectrogram (from anodes 8 and 9) shows high counts at energies extending up to the maximum observed by IES (18 keV/*e*). At these same times similar signals, but at much lower energies (a few hundred eV), are observed in anodes 0 and 1. As will be shown by Figure 3, anodes 8 and 9 look

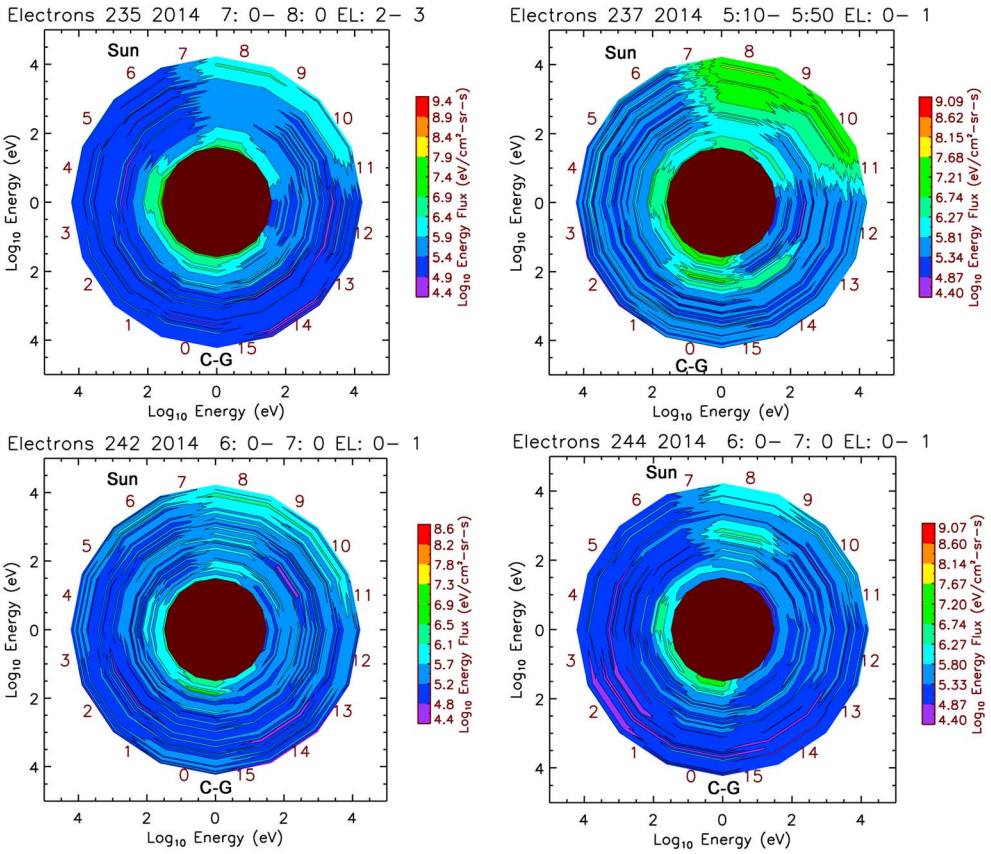

Figure 3. Contour plots of negative particle energy flux for 1 h periods on 23 August (day 235), 30 August (day 242), and 1 September (day 244) 2014 and for a 40 min period on 25 August (day 237) 2014. Anode numbers are noted along with notations of anode viewing angles toward the Sun and the comet (C-G).

generally, but not exactly, toward the Sun while anodes 0 and 1 view toward the comet in azimuth but not in elevation angle, which can be up to 90° off the S/C-comet line.

Figure 3 shows contour plots of energy flux for the nanograin events on 23, 25, and 30 August and 1 September 2014. All of these events are similar in that Rosetta was positioned on the dayside at 50–60 km from the comet. Each contour plot is for the elevation angles for which the most energetic nanograin signal was most prominent. Within the elevation angle range plotted, the positions of the Sun and the comet along the cone of observation are noted, as are the view angles of the 16 different polar angle anodes. As noted before, the angular scan of IES at a given elevation angle is not a 2-D fan except for the midrange elevation angles. For the extreme elevation angles, e.g., channels 0 and 15, the angular scan is along the surface of the 45° half-angle cone [*Burch et al.*, 2007]. In each of the contour plots in Figure 3, there is a strong signal at the highest IES energies, which is located approximately at anode 8. The direction to the Sun is positioned near anode 6 or 7 in each case. This angle of arrival of the negative particles with respect to the solar direction is similar to that observed for pickup ions near comet 67P [*Goldstein et al.*, 2015], which is interpreted as resulting from the orientation of the interplanetary magnetic and electric fields. This observation suggests that pickup of the nanograins by the solar wind is important in addition to the effects of radiation pressure as described by *Horányi and Mendis* [1985]. Near the direction to the comet a signal at energies of a few hundred eV is noted in each case just outside the black region, which extends out to ~32 eV. This black region results from the exclusion of data at the lower energies, which include high fluxes of solar wind and ionospheric or coma electrons. In addition to the signal from the comet direction, similar signals are seen in each case in anode 4, which views a direction intermediate between the comet and the Sun. It is possible that these signals are associated with the interplanetary magnetic field (IMF) direction although this possibility cannot be confirmed with the currently available data.

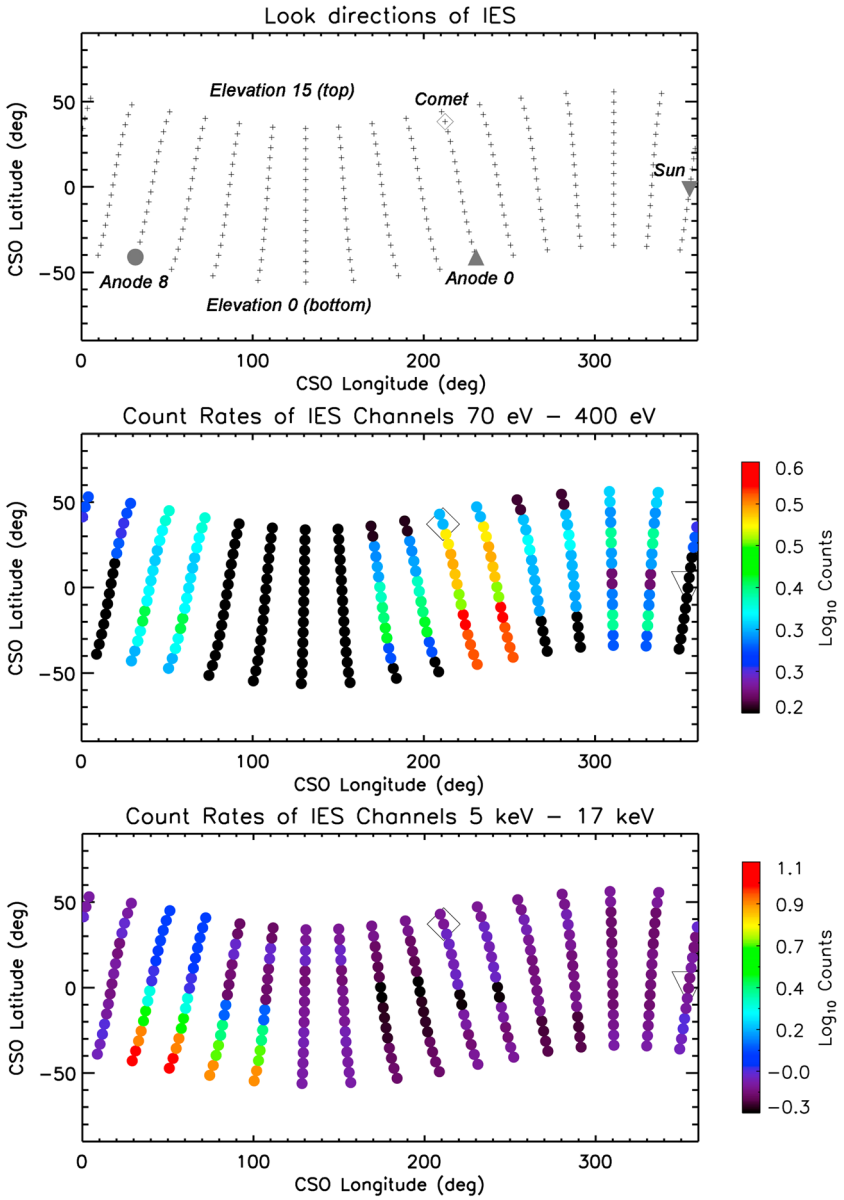

Figure 4. (top) Viewing directions of the IES electron channels (elevation and azimuth) in the CSO (comet solar orbital) coordinate system. (middle and bottom) Median counts per 0.38 s for each channel pair (adjacent elevation and azimuth channels are averaged) for the time period 05:10 to 05:50 UT on 25 August 2014 are shown by the colors of the data points, which are located at the center of each channel's field of view.

In order to aid visualization of the geometry of the observations, the look directions of the 256 IES channels are shown in Figure 4 (top). Also shown are the directions to the Sun and the comet in the CSO (comet solar orbital) coordinate system (right-handed system with origin at the comet, 0° longitude toward the Sun, and latitude measured northward from comet orbital plane, which is inclined by 7.05° to the ecliptic plane). The data points shown in Figure 4 (middle and bottom), which locate the centers of the fields of view of each channel, are color coded by the mean count rate over selected energy/charge ranges—70 eV to 400 eV in Figure 4 (middle) and 5 keV to 17 keV in Figure 4 (bottom). Figure 5 shows that the lower energy nanograins (in the 100 eV range) were arriving from a narrow range of CSO longitudes aligned with the position of the comet. However, the grains arrive over a wide range of latitudes, and the energy dependence of the latitude variation is explored in the next paragraph. Figure 4 also confirms that as shown in Figure 2, the high-energy particles arrived from roughly the solar direction but offset from it as would be expected for particles picked up and energized by the solar wind.

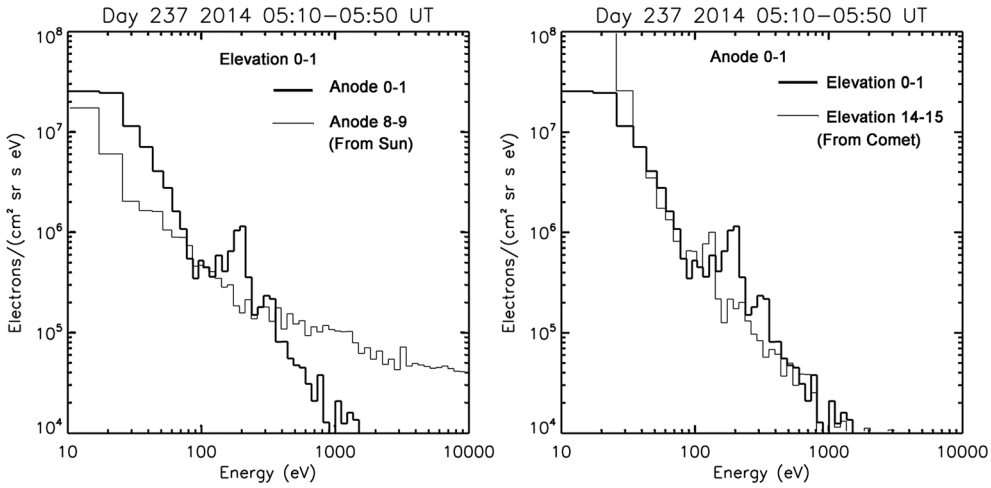

Figure 5. Energy spectra for negative particles (electrons below about 70 eV and nanograins for higher energies) (a) for two anode channels at elevation channels 0–1, which are shown in the contour plot in Figure 2 for day 237 (25 August) 2014, and (b) for two elevation channels at anode channels 0–1, which view in the direction of the comet at elevation channels 14–15.

Energy spectra of the negative particles for the observations on 25 August for elevation channels 0–1 and anodes 8–9 (approximately coming from the Sun) and anodes 0–1 (coming approximately from the comet in CSO longitude but inclined in latitude as shown in Figure 4) are shown in Figure 5 (left). The heavy trace is for negative particles coming from the comet's longitude but displaced in latitude, while the light trace shows particles coming from approximately the solar direction (see Figure 4). While the returning particles (primarily picked up by the solar wind) show a broad, mostly featureless energy spectrum extending through the highest IES energy channels, the outflowing particles have lower energies with distinct peaks in the energy range around 100 eV. These peaks are similar to those observed by *Hill et al*. [2012] in the Enceladus plume that were interpreted to result from grains of different masses being sampled by the rapidly moving Cassini spacecraft. If, as suggested by *Gombosi et al*. [2015], the nanograins from the comet flow outward in a fairly narrow range of velocities (a few hundred m/s), then the multiple peaks shown in Figure 5 could possibly result from particles with roughly equal masses and velocities but different charge states.

Figure 5 (right) shows the same heavy trace as in Figure 5 (left) along with a light trace, which is the energy spectrum from anodes 0–1 at elevation channels 14–15, which contain the direction closest to that of the comet. The same two energy peaks in the 100 eV range appear in both traces but are at about 40% higher energies in the heavy trace. The source of this latitudinal energy dependence is not known but may be related to acceleration by the solar wind electric field near the comet.

4. Interpretation

Although the data presented herein are from an electron analyzer, the presence of fluxes at energies above 10 keV/*e* indicates that heavier particles such as negative ions or charged nanograins (possibly clusters of ions) rather than electrons are being detected. Solar wind electrons, photoelectrons, and coma electrons are all at much lower energies (well below a few hundred eV). Because of the occasional and very localized nature of the negative particle signatures and their point of origin in the neck region of the comet, from which active plumes often originate, we conclude that they most likely are cometary particles or grains that pick up electrons during their motion through the photoelectron and coma electron environment close to the comet rather than atmospheric species ionized by electron attachment (i. e., negative ions). This conclusion is further supported by the fact that previous observations of negative ions from comets have been of thermal ionospheric (coma) ions, which obtained their observed energies by the high velocity of a flyby spacecraft such as Giotto [e.g., *Chaizy et al*., 1991]. Moreover, since the terminal velocity of dust or grains from the comet is expected to be a few hundred m/s [cf. *Gombosi et al*., 1986, 2015] the observed energies of particles coming from the nucleus imply masses of $>10^5$ amu/*e*.

5. Discussion and Conclusions

The Rosetta IES data presented in this study represent the first measurements of energetic charged submicron-sized dust or ice grains (nanograins) in a cometary environment. Previous measurements of charged nanograins at Enceladus [*Hill et al*., 2012] and at comet Halley [*Sagdeev et al*., 1989] were of generally stationary particles whose energies in the measurement frame resulted from high spacecraft velocities. For Rosetta the very low velocities with respect to the comet (a few m/s) along triangular trajectories 50–60 km from the comet in the sunward direction provided a unique opportunity to observe charged nanograins ejected from the comet as well as their predicted reflection by solar radiation pressure and solar wind electric fields [*Mendis and Horányi*, 2013; *Mann et al*., 2014].

As comet 67P and Rosetta complete their journey around the Sun and again move to larger distances, we anticipate more instances of the favorable triangular trajectories upstream of the comet, which again will provide optimal viewing of nanograins as they leave and return to comet 67P. During these future studies we expect to search for collective plasma effects produced by the dust, perhaps including the dust acoustic waves predicted by *Rao et al*. [1990], through their effects on electron densities. Another future task we are considering is quantitative modeling of the solar wind pickup process using observed IMFs and solar wind velocities to test the plausibility of this mechanism for producing the accelerated and reflected grains.

These future observations may also provide opportunities to investigate possible effects of the nanograins on ambient electron densities as suggested by *Vigren et al*. [2015] and on the effects of nucleus charging on nanograin acceleration as proposed by *Szego et al*. [2014]. These further measurements should also provide the opportunity to search for interplanetary dust blown outward from the Sun as described by *Mann et al*. [2014]. These particles have not been noticed as yet, possibly because their flux levels are below the IES threshold or their energies are above the IES energy range.

Acknowledgments
Rosetta is an ESA mission with contributions from its member states and NASA. The data for this work are available from ESA's PSA archive or NASA's PDS Small Bodies Archive. The work on IES was supported by the U.S. National Aeronautics and Space Administration through contract 1345493 with the Jet Propulsion Laboratory, California Institute of Technology. Work at the University of Michigan was supported by NASA under contract JPL-1266313. We thank the teams at Imperial College London and ESA who have been responsible for the operation of IES. Thanks are due to ESA for providing the navigation camera images and the 3-D nucleus model and trajectory plots.

The Editor thanks two anonymous reviewers for their assistance in evaluating this paper.

References

Burch, J. L., R. Goldstein, T. E. Cravens, W. C. Gibson, R. N. Lundin, C. J. Pollock, J. D. Winningham, and D. T. Young (2007), RCP-IES: The ion and electron sensor of the Rosetta Plasma Consortium, *Space Sci. Rev.*, *128*(1), 697–712, doi:10.1007/s11214-006-9002-4.

Burch, J. L., T. E. Cravens, K. Llera, R. Goldstein, P. Mokashi, C.-Y. Tzou, and T. Broiles (2015), Charge exchange in cometary coma: Discovery of H^- ions in the solar wind close to comet 67P/Churyumov-Gerasimenko, *Geophys. Res. Lett.*, *42*, 5125–5131, doi:10.1002/2015GL064504.

Chaizy, P., et al. (1991), Detection of negative ions in the coma of Comet P/Halley, *Nature*, *349*, 393–396.

Edberg, N. J. T., et al. (2015), Spatial distribution of low-energy plasma around comet 67P/CG from Rosetta measurements, *Geophys. Res. Lett.*, *42*, 4263–4269, doi:10.1002/2015GL064233.

Goldstein, R., et al. (2015), The Rosetta Ion and Electron Sensor (IES) measurement of the development of pickup ions from comet 67P/Churyumov-Gerasimenko, *Geophys. Res. Lett.*, *42*, 3093–3099, doi:10.1002/2015GL063939.

Gombosi, T. I., A. F. Nagy, and T. E. Cravens (1986), Dust and neutral gas modeling of the inner atmospheres of comets, *Rev. Geophys.*, *24*, 667–700, doi:10.1029/RG024i003p00667.

Gombosi, T. I., J. L. Burch, and M. Horányi (2015), Negatively charged nano-grains at 67P/Churyumov-Gerasimenko, *Astron. Astrophys.*, doi:10.1051/0004-6361/201526316.

Hill, T. W., et al. (2012), Charged nanograins in the Enceladus plume, *J. Geophys. Res.*, *117*, A05209, doi:10.1029/2011JA017218.

Horányi, M., and D. A. Mendis (1985), Trajectories of charged dust grains in the cometary environment, *Astrophys. J.*, *294*, 357–368, doi:10.1086/163303.

Köhnlein, W. (1996), Radial dependence of solar wind parameters in the ecliptic (1.1 $R_\odot$–61 AU), *Sol. Phys.*, *169*, 209–213, doi:10.1007/BF00153841.

Mann, I., N. Meyer-Vernet, and A. Czechowski (2014), Dust in the planetary system: Dust interactions in space plasmas of the solar system, *Phys. Rep.*, *536*(1), 1–39, doi:10.1016/j.physrep.2013.11.001.

Mendis, D. A., and M. Horányi (2013), Dusty plasma effects in comets: Expectations for Rosetta, *Rev. Geophys.*, *51*, 53–75, doi:10.1002/rog.20005.

Rao, N., P. K. Shukla, and M. Y. Yu (1990), Dust-acoustic waves in dusty plasmas, *Planet. Space Sci.*, *38*, 543–546, doi:10.1016/0032-0633(90)90147-I.

Sagdeev, R. Z., E. N. Evlanov, M. N. Fomenkova, O. F. Prilutskii, and B. V. Zubkov (1989), Small-size dust particles near Halley's comet, *Adv. Space Res.*, *9*, 263–267, doi:10.1016/0273-1177(89)90272-X.

Szego, K., A. Juhász, and Z. Bebesi (2014), Possible observation of charged nanodust from comet 67P/Churyumov–Gerasimenko: An analysis for the ROSETTA mission, *Planet. Space Sci.*, *99*, 48–54.

Tapley, B. D., B. E. Schutz, and G. H. Born (2004), *Statistical Orbit Determination*, pp. 29–32, Elsevier Academic Press, Burlington, Mass.

Vigren, E., M. Galand, P. Lavvas, A. I. Eriksson, and J.-E. Wahlund (2015), On the possibility of significant electron depletion due to nanograin charging in the coma of comet 67p/Churyumov-Gerasimenko near perihelion, *Astrophys. J.*, *798*, 130, doi:10.1088/0004-637X/798/2/130.